Journal of Coastal Research	00	0	000–000	Coconut Creek, Florida	Month 0000

A Model for Simulating Barrier Island Geomorphologic Responses to Future Storm and Sea-Level Rise Impacts

Heng Dai[†], **Ming Ye**[†*], **and Alan W. Niedoroda**[‡]

[†]Department of Scientific Computing and Geophysical Fluid Dynamics Institute
Florida State University
Tallahassee, FL 32306, U.S.A.

[‡]Wyndham Consultants, LLC
Tallahassee, FL 32312, U.S.A.

ABSTRACT

Dai, H.; Ye, M., and Niedoroda, A. W., 0000. A model for simulating barrier island geomorphologic responses to future storm and sea-level rise impacts. *Journal of Coastal Research,* 00(0), 000–000. Coconut Creek (Florida), ISSN 0749-0208.

This paper presents the Barrier Island Profile (BIP) model, a new computer code developed to simulate barrier island morphological evolution over periods ranging between years and decades under the impacts of accelerated sea-level rise and long-term changes in the storm climate. The BIP model is a multiline model that represents the time-averaged dynamics of major barrier island features from front beach to backshore. Unique contributions of BIP to coastal modeling include a dynamic linking of interacting barrier island features and consideration of both future sea-level rise and storm climate impacts. The BIP model has the built-in capability of conducting Monte Carlo (MC) simulations to quantify predictive uncertainty caused by uncertainty in sea-level rise scenarios and storm parameters. For a series of barrier island cross-sections derived from the characteristics of Santa Rosa Island, Florida, BIP was used to evaluate their responses to random storm events and five potential accelerated rates of sea-level rise projected over a century. The MC simulations using BIP provide multiple realizations of possible barrier island morphologic responses and their statistics, such as mean and variance. The modeling results demonstrate that BIP is capable of simulating realistic patterns of barrier island profile evolution over the span of a century using relatively simple representations of time- and space-averaged processes with consideration of uncertainty of future climate impacts.

ADDITIONAL INDEX WORDS: *Beach sand dunes, storm erosion, sediment transport, overwash, Monte Carlo, uncertainty analysis, SLOSH, Santa Rosa Island.*

INTRODUCTION

In response to impacts of future storms and sea-level rise, coastal planners and engineers are making accommodations in their management plans for protection of coastal infrastructure and natural resources. Barrier islands are important for coastal protection and restoration, and they have been well studied. However, little attention has been given to the balance of processes and sand transport fluxes that combine to shape the composite morphology. The principal morphological elements include the beach prism, the frontal and secondary dunes, the overwash channels, the island platform, and the back-island shoreline. Understanding the balance of these time-averaged processes and representing them in a quantitative framework is especially of value when this can be used to forecast decadal- and century-scale evolution of a barrier island system as a whole. The morphology of barrier islands will be dramatically affected by the future climate, including storms and sea-level rise. Accurately predicting the morphological evolution of barrier islands is necessary for coastal management, and mathematical modeling is a vital tool for such predictions. This paper presents a barrier island profile (BIP) model with consideration of future uncertainty for simulating barrier island morphological evolution with multiple features such as beach, dunes, island platform, and backshore under both long-term and short-term climate impacts including uncertain sea-level rise and storms.

A number of recent studies of changes in barrier island morphology as it has reacted to, and recovered from, the devastation wrought by major hurricanes have provided insight into the major factors to consider in developing a conceptual model of the linkages between morphological features and the processes that shape them. Morton (2002) has identified the principal factors influencing storm impacts as being the characteristics of the storm or storm sequence, the location of barrier island features relative to the storm track and point of landfall, the sequencing of storms over time, and the height and duration of storm surge flooding, along with the antecedent topography and framework geology. Several studies describe differences in storm impact and poststorm recovery along individual barrier island systems, providing insight into the interaction between morphological features. It has long been accepted that storm overwash, which transports sand from the beach prism through the dunes to be deposited on the island platform and along the island backshore, is key to sustaining barrier islands, especially in the presence of sea-level rise (Godfrey and Godfrey, 1976). Houser and Hamilton (2009) and Timmons *et al*. (2010), among others, have noted a relationship between the stability of the island backshore and the width of the island. Wider barrier islands limit or prevent overwash from being carried completely across the island to the backshore beach. If the barrier island is transgressive, this leads to erosion of the backshore and a tendency for the island width to decrease over time. Timmons *et al*. (2010) describe how this leads to a

DOI: 10.2112/JCOASTRES-D-14-00094.1 received 12 May 2014; accepted in revision 16 October 2014; corrected proofs received 25 November 2014; published pre-print online 31 December 2014.
*Corresponding author: mye@fsu.edu

tendency for transgressive barrier islands to develop a certain stable width and to maintain it as they retreat.

The development of individual morphological features on barrier islands is often controlled by a complex combination of processes and factors. The general shape of the island is controlled by some processes that act slowly and continuously. This is best exemplified by longshore sand transport along the beaches and adjacent surf zones. Subtle spatial gradients in the long-term time-averaged rates of longshore sand transport lead to chronic patterns of erosion and deposition. Major storms generally produce sudden and acute changes in the beach prism, dunes, and island platform. It is challenging to consider all the processes of different time and space scales in coastal morphological modeling.

An approach to address this challenge is to match the time and length scales of the processes being modeled, as recognized by Stive and De Vriend (1995). In this context, this study uses the long-term modeling approach. The basic idea of the approach is that the interaction of a large number of processes and mechanisms acting over a variety of time and space scales determine coastal morphological behaviors, as described in several papers (e.g., De Vriend, 1991; De Vriend *et al*., 1993; Stive, Nicholls and De Vriend, 1991). This avoids the need to include mathematical representations of too many detailed effects and processes. Instead, once the proper scales of the system to be represented are determined, then the dominant processes can be identified. Processes and effects that occur at smaller time or length scales are generalized and usually represented by simplified parameterizations. A good example is the way that turbulence is treated in many hydrodynamic models. Rather than attempting to represent the rapidly fluctuating speeds and directions of the fine-scale flow, the overall effect of these eddies on the mean flow is represented by turbulent eddy coefficients. Also, processes operating at time and length scales greater than those of interest are treated as external forcings.

In order to produce a numerical model that represents the long-term response of barrier islands to accelerated sea-level rise and variations in the storm climate it is necessary to first develop a conceptual model. In the present case it has been necessary to exploit a first-order difference between the system processes that dominate longshore profile changes and those that control cross-shore profile changes. A complete model would include both, along with their interactions. However, the process for developing such a model can be facilitated by, and much can be learned from, the development of a model such as the BIP that only represents cross-shore processes because it captures the acute storm-dominated morphological changes.

The BIP model represents the morphological development of barrier island systems on time scales of years to centuries and length scales of tens to hundreds of kilometers. Five different century-long sea-level rise scenarios are defined as external forcing. Each of the major elements of the overall generalized island morphology is represented and linked to the adjacent elements, but internal boundary conditions are defined by the time-averaged sediment volume flux. The model is forced by representations of a series of hurricane simulations drawn from a statistical characterization of the storm climatology that is representative of the NE Gulf of Mexico. The simulation of each hurricane includes determination of the maximum height, duration of the storm surge, and the corresponding wave conditions. The hurricane intensity and the distance between each profile and the point of landfall are determined in a random manner, while the annual rate of storm occurrence is defined by a Poisson distribution. Multiple realizations of 100-year-long sequences of these synthetic hurricanes are then used to statistically define the resulting changes in barrier island profiles. This, in turn, provides the information needed to characterize the mean, variability, and uncertainty associated with each of the modeled scenarios.

This paper describes the mathematical representations of the time- and space-averaged sediment transport processes and how they are linked. The generalized representation of hurricanes and the hurricane storm surges are then defined. Results from simulations of individual 100-year realizations are presented to demonstrate and diagnose the details of the changes in the morphological components resulting from the five different sea-level rise scenarios. Results from the simulations of multiple realizations (1000) of century-long storm sequences are then given, and the statistical characterizations of these results are described. The use of these results in characterizing uncertainty is then described.

METHODS

This section first describes the conceptual–mathematical model on which BIP computer code was developed. An example BIP modeling outcome is then presented to simulate the geomorphologic response to future storms and different rates of sea-level rise over a 100-year period.

The BIP Model

In the BIP model, barrier island morphology is represented as a set of width-averaged cross-sections or profiles, each of which include beach dune, front beach, island platform, and backshore. Sea-level rise affects the elevation of the entire profile except that of the front beach; it is assumed that the front beach elevation changes with sea-level rise, as will be discussed later. In addition to the shape of the beach prism and dunes, storms affect the island platform and backshore through dune erosion and redistribution of eroded sand volume to the island platform and backshore. The details of how barrier island components and processes are conceptualized and handled in the BIP model are described below.

Island Profiles

The barrier island morphological evolution in the BIP model is simulated along width-averaged shore-normal profiles. In other words, rather than using specific topographic profiles, the model depends on a generalized representation of the morphological features within wide bands that run across the island (the width of the profiles is an input parameter). The generalized topography within these bands is used to represent a composite of the features in a schematic format. Figure 1 provides a width-averaged, schematic barrier island profile with only one primary dune. For each profile, the beach has a sloped face intersecting the mean water level at location *Yoff*. The beach has a berm and back-beach platform ending at the dune base. The beach berm and back-beach platform intersect the dune face at *DBoff*. The height of the berm and platform is

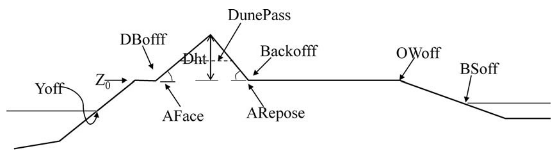

Figure 1. Generalized barrier island profile showing island features from the gulf to the backshore with a single dune.

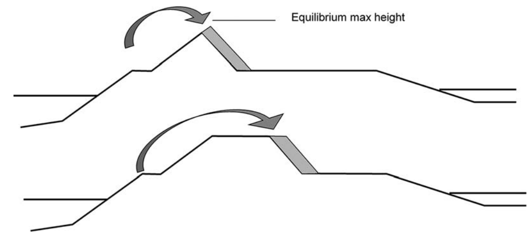

Figure 2. Illustration of annual growth of dune (upper) and dune field (lower) after dune height reaching the predetermined maximum height.

specified relative to mean sea level at dune foot (Z_0). The dune is represented as a ridge characterized by the dune base between *DBoff* and *Backoff* and by seaward face slope (*AFace*) and slip face angle (*ARepose*). The slopes are thought to remain constant as the dune volume varies through changes of *Dht* and *Backoff* caused by sand transport from the beach prism. To account for the ranges of dune heights that are characteristic of individual coastal reaches, the initial dune heights are defined from measured values of the modeling areas. A maximum dune height, which can be determined from measurements of representative profiles of the modeling areas, is needed to model dune growth from a single dune to dune field. When a growing dune reaches this maximum height in the BIP model, a secondary dune is assumed to develop. Rather than using detailed representations of profiles with secondary or even more complex fields of dune ridges, a generalized storage volume is created as a dune field. The dune field geometry is characterized as a trapezoid, and its height is the same as the maximum dune height of the frontal dune ridge. After the height is reached, the storage volume is controlled by the horizontal length of the top of the trapezoid. The transition between a single dune and a dune field depends on the sediment transport, which is described in detail below. Dune passes are located along the dune ridge in the direction perpendicular to the cross-section as shown in Figure 1. The primary dune ridge is represented as a long ridge breached at intervals of dune passes. The dune passes work as sediment transport channels and provide a mechanism for beach sand to be carried across the primary dune ridge to the backshore platform during surge events of major storms such as hurricanes. An island platform (barrier flat) extends from the dune slip face to the backshore at the bay. The platform elevation does not increase with sea-level rise. For example, the elevation is relative to mean sea level and decreases when sea level rises. In the generalized barrier island profile (Figure 1), the island platform freeboard ends at *OWoff*; a gentle slope beyond *OWoff* represents the backshore shoreline characterized by the mean water line (*BSoff*).

Beach Prism

The first morphological feature considered in the BIP model is the front beach prism. While in reality the beach prism changes on a time scale of days to weeks as a result of changes in wave and tide conditions, these variations are not resolved in BIP, and their locations are represented by their annual-average positions. The short-term sand volume exchanges between the beach prism and offshore bars are assumed to be balanced on annual time scales. Because the short-term cycle of sand volume exchange between the beach prism and offshore sand bars is relatively rapid, it is assumed that the vertical elevations of beach face and berm height (Z_0) track the slowly changing mean sea level. In other words, the beach prism rises at the same rate of sea-level rise. Heights of all other elements of the barrier island are dynamic and not tied to sea-level rise. Their elevations and horizontal extents are controlled by deposition from the accumulation in the time-averaged sand volume fluxes.

Barrier Island Dune Ridge

The beach dune or foredune is another important barrier island feature that largely affects the impact of a storm on the barrier island morphology (Houser and Hamilton, 2009). Two dune evolution mechanisms are considered in the BIP modeling: dune recovery and storm-induced dune erosion. The BIP model first needs to consider the foredune growth due to the eolian sediment supply from the beach prism (Houser, Hobbs, and Saari, 2008; Morton, Paine, and Gibeaut, 1994; Stone *et al.*, 2004). Although the eolian sediment transport distribution is a function of wind angle, critical fetch, and beach geometry (Bauer and Davidson-Arnott, 2002), the BIP model focuses on large-scale island profile modeling and it does not take into account the complicated wind-driven microscale and mesoscale sediment transport processes. A generalized sediment transportation rate is used to represent the eolian sediment supply from the beach to the dunes, and it is treated as a flexible model input parameter, which can be easily modified if necessary. As shown in Figure 2, the entire volume is added to the dune face by adjusting the dune height (*Dht*) and width (between *DBoff* and *Backoff*) but keeping *AFace* and *ARepose* as constants. In other words, the dune shape does not change with its increasing volume.

In addition to the dune growth, storm-induced dune erosion is another important dune evolution mechanism considered in the BIP model. During storms, the waves may impact and erode the foredune when high water level occurs (Hanson, Larson, and Kraus, 2010). The research into dune morphologic responses to the storms has demonstrated the devastating effect of storms on foredunes (Houser, Hapke, and Hamilton, 2008). To simulate the dune erosion, a generalized storm wave impact dune erosion rate is used in the BIP model to represent the dune erosion process, and its value is estimated using the algorithms developed in Larson, Erikson, and Hanson (2004) and Larson, Kraus, and Connell (2006):

$$\Delta V_E = 4C_s(R + \Delta h - Z_0)\frac{t}{T}, \qquad (1)$$

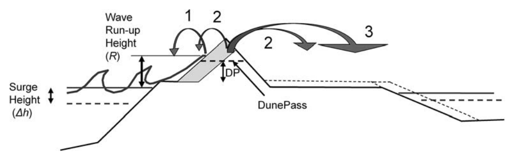

Figure 3. Three mechanisms of partitioning eroded dune sand. Three possible processes are considered: (1) all the eroded sediment is deposited on the beach prism; (2) the eroded sediment is partitioned and deposited on the island platform and the beach prism; (3) all the eroded sediment is deposited on the island platform and backshore.

where ΔV_E [L^2] is the volume of dune eroded per unit profile width (i.e., beach length), C_s [L] is a coefficient with a range between 1×10^{-3} and 2.5×10^{-3}, R [L] is the wave bore run-up height, Δh [L] is the surge height, Z_0 [L] is the elevation difference between the dune foot and the mean water line, t [T] is the surge duration in which $R + \Delta h$ is above Z_0 (a minimum elevation necessary to cause the wave run-up to reach the primary dune), and T [T] is the period of the deep water wave. Since the western panhandle coast at NW Florida is microtidal and wave dominated (Kish and Donoghue, 2013), the astronomical tide is not considered in the dune erosion calculation due to its small magnitude. However, it can be easily added as an adjustment to the surge height and duration of the dune erosion. Although some research has pointed out that vegetation plays an important role in dune size (Duran and Moore, 2013), this research doesn't consider vegetation as a factor.

Wave Parameters Estimated Using SLOSH

The National Oceanic and Atmospheric Association (NOAA) sea, lake, and overland surges from hurricanes (SLOSH) model (Jelesnianski, Chen, and Shaffer, 1992) can be used to estimate the run-up height (R), surge height (Δh), surge duration (t), and wave period (T) at the location of the profile relative to the orientation and landfall location of the storm track. SLOSH takes the user-determined inputs of a storm, including the central pressure drop (Δp); the storm moving velocity (V_F); a coefficient α, which depends on the forward speed of the hurricane and the increase in effective fetch length because the hurricane is moving; and the storm track. The outputs of SLOSH include maximum wind radius (A), maximum wind speed ($U_{\max}$), and maximum surge height that is taken as Δh. According to the Shore Protection Manual (USACE, 1984), the SLOSH inputs and outputs can be used to evaluate the deep water period,

$$T = 8.6e^{\frac{A\Delta p}{100}}\left[1 + \frac{0.104\alpha V_F}{\sqrt{0.865 U_{\max}}}\right], \quad (2)$$

deep water wave height (H_0),

$$H_0 = 16.5e^{\frac{A\Delta p}{100}}\left[1 + \frac{0.208\alpha V_F}{\sqrt{0.865 U_{\max}}}\right], \quad (3)$$

and deep water wave length (L_0)

$$L_0 = \frac{g}{2\pi}T. \quad (4)$$

Variables H_0 and L_0 are used to estimate the wave bore run-up height via (Larson, Kraus, and Connell, 2006),

$$R = 0.10\sqrt{H_0 L_0}. \quad (5)$$

Variable t in Equation (1) is estimated as the period in which $R + \Delta h$ is larger than Z_0 in an assumed sine function of surge height, whose amplitude is $R + \Delta h$ and whose period is the surge duration, t.

Overwash Sediment Distribution to Island Platform and Backshore

Behind the foredunes, the back-barrier area includes the barrier flat (or island platform) and the back-barrier bay (or backshore). Their morphology can be dramatically impacted by washover, which is defined as the sediment transported inland caused by overwash events (Donnelly, Kraus, and Larson, 2006). The overwash is the water and sediment flow going over the beach crest to the back-barrier area driven by storm surge or wave run-up (Carruthers *et al*., 2013). In the BIP model, the washover sediment is from the storm-eroded dune volume, and the dune pass is the overwash channel as described above. Three mechanisms in BIP are considered to determine the location where the overwash of eroded dune volume (ΔV_E) is deposited. These mechanisms determine the fate of overwash sediment based on the values of surge height, wave run-up height, dune height, and dune pass elevation. In the first mechanism, as shown in Figure 3, if the sum ($\Delta h + R$) of run-up height and surge height is smaller than the sum ($Z_0 + Dp$) of dune foot and dune pass height, all of the eroded dune volume deposits on the beach prism. If $\Delta h + R$ is larger than $Z_0 + Dp$ but smaller than the sum ($Dht + Z_0$) of dune height and dune foot, then the eroded volume is partitioned between the beach prism and the overwash. The portion of sand returning to the beach prism is determined by the empirical ratio between excessive run-up height (relative to the dune pass) and the difference between dune height and dune pass height

$$P = (R + \Delta h - Z_0 - Dp)/(Dht - Dp). \quad (6)$$

If $\Delta h + R$ exceeds $Dht + Z_0$, then all of the eroded volume is carried beyond the dune by overwash and deposits on the island platform. The overwashed sand in the latter two mechanisms is assumed to be deposited uniformly across the island platform, leading to increased island platform freeboard. When the computed elevation of the island platform equals or exceeds the elevation of the dune foot (Z_0), the excessive volume is not used to increase the island platform height. Instead it is transferred to the backslope of the island and is uniformly distributed there. This, in turn, displaces the backshore shoreline position outward into the bay.

Multiple Simulations Capability

Since a single simulation of future conditions is of limited value when dealing with a natural coastal system that is strongly forced by a highly variable set of storms, the BIP model is designed to have the built-in ability to generate multiple sequences of random storms and to conduct Monte Carlo (MC) simulations for quantifying the uncertainty of large-scale barrier island evolutions with the space scale of tens of kilometers and the time scale of decades or centuries. The model generates random numbers of storm-related variables (i.e., numbers, magnitudes, and tracks) and considers multiple

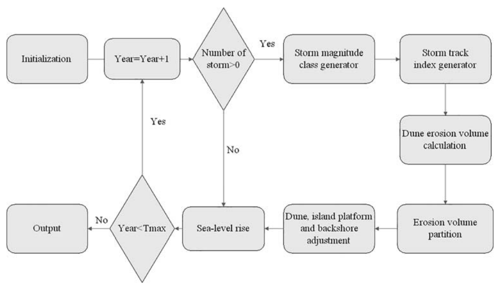

Figure 4. Flowchart of the BIP model simulation of barrier island geomorphologic responses to future storm and sea-level rise impacts.

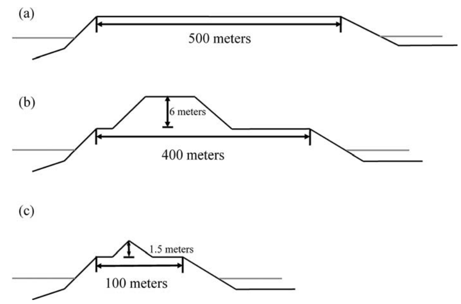

Figure 5. Three semisynthetic barrier island profiles: (a) no initial dune and long island length, (b) large initial dune field and relatively short island length, and (c) small initial dune with short island length.

sea-level rise scenarios. The model outputs not only include individual realizations of barrier island evolution but also the statistics (e.g., mean, variance, and probability density function) based on the realizations. These statistics can be used for science-based decision-making for coastal management and planning.

Model Flowchart

Figure 4 shows the flowchart of the BIP model single run. It starts with initializing the morphology of the profiles. The time step is normally set at one year. In each time step, random storm conditions (i.e., numbers, tracks, and magnitudes) are generated. For each storm, a random storm track and a storm magnitude are generated. Using these storm parameters, the volume of dune erosion is computed for each storm using Equation (1). Subsequently, the erosion volume is partitioned according to the three mechanisms discussed above to adjust heights of dune, platform, and backshore. Regardless of the occurrence of storms, dune annual growth and sea-level rise are incremented each model year.

Modeling Example

An example of BIP modeling (including a Monte Carlo simulation) was conducted to simulate geomorphologic response of three semisynthetic barrier island profiles to future storms and five different rates of sea-level rise over a 100-year period. The details of the modeling example are given below.

Semisynthetic Profiles

The dimensions of the beach, sand dune, island platform, and island width of the schematic width-averaged profiles represent three semisynthetic profiles across Santa Rosa Island (Figure 5) located mainly in Okaloosa County of West Florida Central Panhandle Coast. This island hosts the military infrastructure of Eglin Air Force Base and is largely undeveloped and with a well-studied geomorphology (Claudino-Sales, Wang, and Horwitz, 2008; Kish and Donoghue, 2013; Miller *et al*., 2014; Wang *et al*., 2006). It protects the mainland infrastructure of the base from cyclonic storms. Figure 6 shows two topographic profiles across natural portions of the island, and they provide representative dimensions for the dune, dune field, and island profiles used in the BIP model application. Each profile has a constant width of 250 m (perpendicular to the profiles), and the initial elevation of the island platform has been simplified to a constant of 2 m above mean sea level. Profile 1 in Figure 5a has a cross-island length of 500 m with no dune on it initially. Profile 2 in Figure 5b is 400 m long with a dune field that is initially 6 m high and 32 m long across the island. The initial length of profile 3 in Figure 5c is 100 m, and the initial dune height and length are 1.5 and 7 m.

Model Parameters

The annual rate of eolian sand transport toward the dunes from the beach is one of the most important parameters in the BIP model. The beach nourishment feasibility study for Okaloosa County by Taylor Engineers (2007) studied the sediment transported through winds at the Santa Rosa Island area. They applied the method outlined in the Coastal Engineering Manual (CEM; USACE, 1998) for wind-blown sediment transport through the turbulent kinetic energy relationship, which calculates the sediment transport mass rate using wind shear velocity and sand grain size. By using the wind speed data obtained from the study area to estimate the wind shear velocity, they calculated the sediment transport rate at the coastal zone at Santa Rosa Island area. The calculated onshore sediment transport rate of 1.3 m^3/m/y presented in the Taylor report can be used as a representation of eolian sediment transport from beach to the dunes for the BIP model. The empirical coefficient, C_s, value needed to evaluate Equation (1) of dune erosion was chosen using the mean value in research of Larson, Erikson, and Hanson (2004) as 1.8×10^{-3}.

In the SLOSH modeling needed for evaluation of Equation (1), only hurricanes are considered because lesser storms seldom cause dune erosion in the Florida Panhandle coast. In order to provide computational efficiency it was necessary to avoid making simulations with SLOSH for all possible hurricane conditions. Instead, a standard set of hurricanes, each representing an important intensity class, was developed based on Federal Emergency Management Agency (FEMA) coastal flood studies for Okaloosa County (FEMA Staff, 2002). This set was used as a catalog of baseline storms, and each was modeled with SLOSH to determine the maximum wind radius, wind speed, and surge height needed to evaluate Equations (2)–(5) for the SLOSH modeling domain. Based on these results, the variables needed to evaluate Equation (1) were selected for the profiles according to the distance and locations

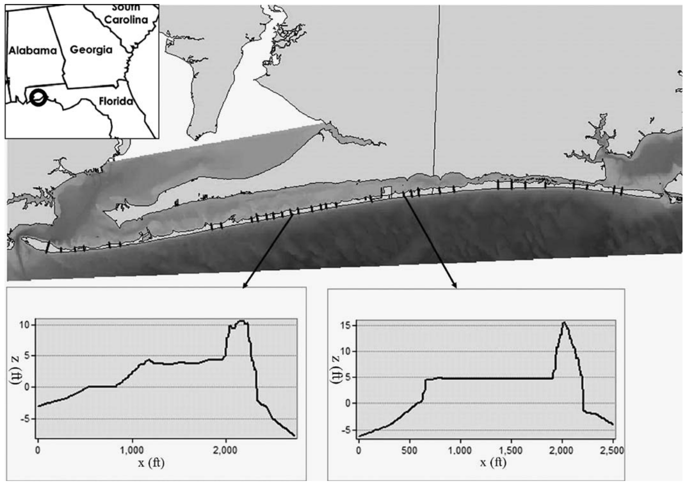

Figure 6. Regional (top left corner) and local maps of Santa Rosa Island (top), and characteristic topographic profiles of a dune field (bottom left) and a single dune (bottom right) across natural sections of the island. The bay is on the left and the Gulf of Mexico is on the right of the profiles.

(to right or left) of the storm track landfall relative to the location of the profile being modeled.

Uncertain Storm Parameters

In a model run, as shown in Figure 4, when the storm number is larger than zero, the storm magnitude and storm track (landfall location) are determined for each storm. To allow the storm landfall locations to be at varying distances from each profile, a straight shoreline segment is forged with a length of 45 km, similar to that of the Santa Rosa Island. Only hurricanes making landfall within this zone are considered in the SLOSH modeling. Instead of modeling all possible tracks, three storm tracks were considered. Figure 7 shows the locations of the three profiles relative to the storm tracks, and Table 2 lists the distances between these profiles and landfalls with the different tracks. For the three discrete storm tracks, assuming that the probability of storm occurrence on the tracks follows a uniform distribution, a discrete random number (1, 2, and 3) was generated as the storm track index.

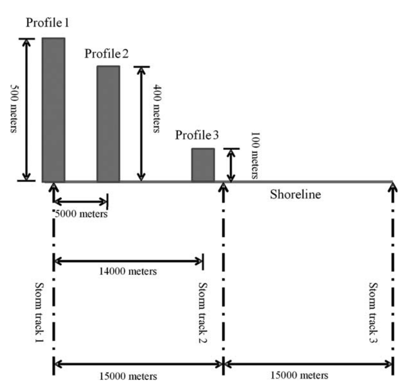

Figure 7. Relative locations of three island profiles (columns) to three storm tracks (dashed arrows).

A random hurricane magnitude is determined using the exceedance probability of maximum storm surge height. Figure 8 shows the probability estimated from the data of the Okaloosa County FEMA Flood Study (FEMA Staff, 2002). Instead of considering all possible hurricane magnitudes, four magnitude classes were used in this study as a practical number, but more classes can be handled by the BIP model. Similar to the storm impact scales proposed by Sallenger (2000), these four different magnitudes of storms were developed to cover different surge and wave run-up heights. In order to focus on sea-level rise impacts during a period of decades to centuries, we preferred to ignore rare events and to consider representative storm classes that are relatively more frequent but with lesser magnitude. Therefore, the storms in this BIP application fall into impact level 2 and level 3 of Sallenger's research (Sallenger, 2000). To demonstrate the three mechanisms of sediment transport described in the methodology section and shown in Figure 3, storm surge elevations ranging from limited beach flooding to severe dune attack were determined using trials and errors. This resulted in selecting storm magnitudes that produce surge heights of 0.3, 0.64, 1.16, and 2.1 m. The exceedance probability (Figure 8) was divided into four intervals, each of which centers on the chosen surge heights. The corresponding cumulative exceedance probability ranges for each class were 0 to 0.5, 0.5 to 0.75, 0.75 to 0.95, and greater than 0.95 (Figure 8). Based on the cumulative probabilities, a discrete random number (1–4) was used to assign one of these storm magnitude classes for each storm represented in the model.

Four SLOSH model runs were conducted for the four storm magnitude using the Panama City (Florida) grid, which includes the Santa Rosa Island. A trial-and-error procedure was followed to set the values of the central pressure of the modeled hurricanes, which resulted in matching the four desired maximum surge heights. Using the distances between storm landfall and the profiles, the maximum surge heights at each profile were determined. For each storm magnitude class

Table 1. *An example of a storm series for a 100-year period of BIP simulation.*

	Year						
	6	16	21	52	70	70	87
Storm number	1	1	1	1	2	2	1
Storm track index	2	1	3	3	2	2	2
Storm magnitude class	2	4	3	1	3	2	1

and each track index, a look-up table was developed to contain the surge heights, maximum wind speed, and deep water wave height and period for each of the profiles, which are needed to evaluate Equations (1)–(5).

In each year of the BIP model, a random storm number, track index, and magnitude class for a period of 100 years were generated. Table 1 lists an example realization. The storm numbers for a given year were generated from the Poisson distribution,

$$P(k;\lambda) = \frac{\lambda^k e^{-\lambda}}{k!}, \qquad (7)$$

where k is the storm number, and λ is the expected occurrence for a period of time. Based on a FEMA study of the West Florida Central Panhandle coast (FEMA Staff, 2002), the annual rate of hurricanes is estimated to be 0.001327 per kilometer of shoreline. This yields an annual storm rate of 0.06 for the shoreline length, meaning that the expected occurrence in the 100-year simulation period is $\lambda = 6$.

Sea-Level Rise Scenarios

Five scenarios of sea-level rise with different rates were considered in the BIP model. The annual sea-level rise increment in each scenario was calculated using the following quadratic equations (NRC, 1987):

$$\begin{aligned}
&\text{Scenario 1 (SLR}+0.15\text{)}: && \mathrm{SLR}_1(i) = (1.5\times10^{-3})i,\\
&\text{Scenario 2 (SLR}+0.50\text{)}: && \mathrm{SLR}_2(i) = (1.7\times10^{-3})i + (3.3\times10^{-5})i^2,\\
&\text{Scenario 3 (SLR}+1.00\text{)}: && \mathrm{SLR}_3(i) = (2.03\times10^{-3})i + (7.97\times10^{-5})i^2,\\
&\text{Scenario 4 (SLR}+1.50\text{)}: && \mathrm{SLR}_4(i) = (2.57\times10^{-3})i + (1.243\times10^{-4})i^2,\\
&\text{Scenario 5 (SLR}+2.00\text{)}: && \mathrm{SLR}_5(i) = (2.57\times10^{-3})i + (1.743\times10^{-4})i^2,
\end{aligned} \qquad (8)$$

where i is the year number and SLR is the sea-level rise (m) at the ith year. The first scenario is a continuation of the present rate of 1.5×10^{-3} m/y, which results in sea-level rise of 0.15 m over the next 100 years; the sea-level rises of the other four rates are 0.50, 1.0, 1.5, and 2.0 m, respectively. The five scenarios cover the full range of recent estimates of sea-level rise, which include 0.18–0.59 m (IPCC, 2007), 0.75–1.90 m (Vermeer and Rahmstorf, 2009), 0.90–1.30 m (Grinsted, Moore, and Jevrejeva, 2010), and 0.6–1.6 m (Jevrejeva, Moore, and Grinsted, 2010). The five scenarios are denoted as SLR + 0.15, SLR + 0.5, SLR + 1.0, SLR + 1.5, and SLR + 2.0, and their corresponding estimates of sea-level rises are illustrated in Figure 9. It should be noted that the BIP model is general and can handle any rates of sea-level rise, not limited to the five rates above.

Table 2. *Distances between three different barrier island profiles and three storm tracks.*

Island profile	Storm track 1 (m)	Storm track 2 (m)	Storm track 3 (m)
1	0	15,000	30,000
2	5000	10,000	25,000
3	14,000	1000	16,000

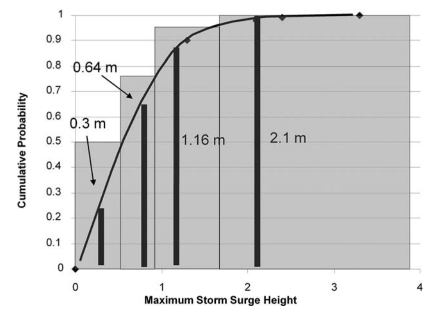

Figure 8. Cumulative probability of maximum storm surge heights (0.3, 0.64, 1.16, and 2.1 m) and their discretization for four selected storm magnitude classes (1–4 from left to right).

RESULTS

The BIP model can be run in two modes: (1) a deterministic run with a single set of storm parameters (i.e., storm number, track, and magnitude) under an individual sea-level rise scenario, and (2) a stochastic run with multiple realization storm parameters and/or under the five sea-level rise scenarios. The first mode is useful for simulating past barrier island evolution for purposes such as model calibration. The second mode is necessary to address uncertainty in the storm parameters and sea-level rise scenarios.

Results from a Deterministic Simulation

The results and discussions in this section are for the single simulation of the storm series listed in Table 1 and sea-level rise scenario SLR + 1.0. For this individual realization, the first storm occurs in the sixth year, and it is the only storm in that year. This storm is of magnitude 2 and travels along the central storm track. Note that, in the seventieth year, there

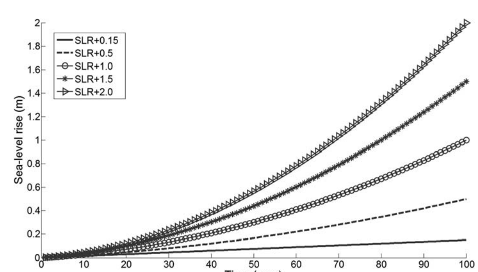

Figure 9. Estimated five sea-level rise scenarios in 100 years used in the BIP model. At the end of 100 years, the sea-level rises are 0.15, 0.5, 1.0, 1.5, and 2.0 m for the five scenarios, respectively.

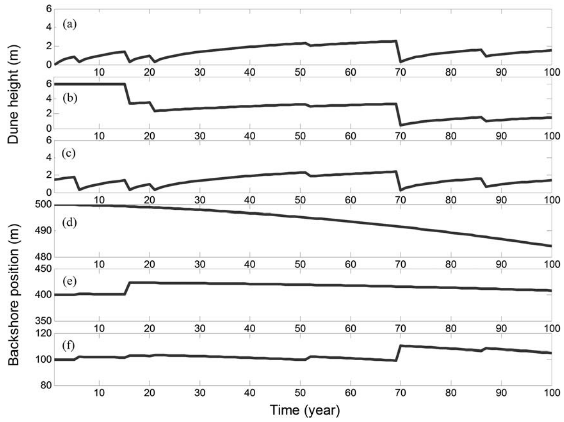

Figure 10. Changes of dune height (a–c) and backshore position (d–f). Panels (a) and (d) are along profile 1, (b) and (e) along profile 2, and (c) and (f) along profile 3.

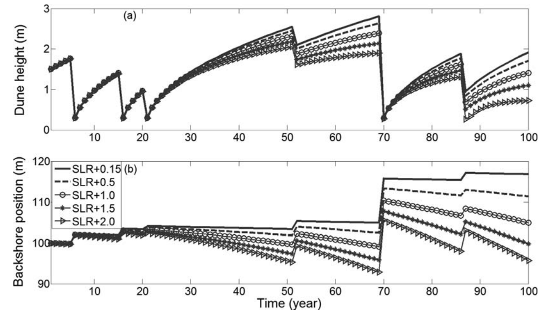

Figure 11. Comparison of responses of (a) dune height and (b) backshore position of profile 3 to five sea-level rise scenarios.

are two storms, which are of magnitude 3 and magnitude 2, respectively, both making landfall at storm track 2.

Figure 10 plots the predicted time series of dune height (*Dht*) and backshore position (*BSoff*) for the three island profiles. The figure illustrates impacts of storms on dune erosion and recovery as well as backshore evolution. For example, Figure 10a of profile 1 and Figure 10c for profile 3 show that the dunes on the two profiles are completely eroded in years 6, 16, and 21, when storms of magnitudes 2, 4, and 3 occur (Table 1). The storms of magnitude 1 in year 52 and 87 have smaller impacts. The changes are the largest in year 70 for all three dunes, since two large storms occur in this single year. The dunes keep growing during the years without hurricanes as a result of the annual-average eolian sand transport. In comparison with Figures 10a and 10c, Figure 10b of profile 2 shows a slightly different pattern in the early time, because there is a dune field along the profile. Although the dune along this profile is eroded by the same sequence of storms, it is never fully erased because of its large volume. These results demonstrate that the BIP model is capable of simulating reasonable results of cycles of destruction and reconstruction. The different dune evolution patterns for the three island profiles indicate the importance of initial dune heights in the dune evolution processes at the first few decades. At this time period, larger dunes or dune fields are more likely to be maintained than smaller ones even with impacts of multiple relatively large storms. But after a certain time (40–50 years), dunes at different profiles tend to converge to similar size. The initial dune height is not an important factor of dune evolution anymore.

The patterns of backshore position evolution are also different along the three profiles. In Figure 10d of profile 1, the long length of this profile traps all of the eroded dune sand on the island platform with none available to balance against the encroachment of the backshore due to the sea-level rise. This leads to a continuous shift of backshore position, which represents backshore erosion. For the second profile, as shown in Figure 10e, the dune field provides a sufficient amount of sand to maintain the backshore, which results in opposing the transgression due to the sea-level rise. However, this only occurs in year 16 when the magnitude 4 storm happens; subsequent storm events do not provide sand to the backshore. This contrasts with the results shown in Figure 10f for the third profile with narrow length. Although the dune at profile 3 is initially small and is erased three times during the first 25 years, its narrow profile length allows the backshore position to keep up with sea-level rise, since the island profile cannot hold much sand. The results show that the barrier island backshore evolution pattern depends on both beach dune and profile length. It suggests that the profiles with relatively large dunes and smaller length have a greater chance to grow in the backshore. On the contrary, when the small dunes are not capable of providing enough sand and the wide island traps the sand, backshore retreats as sea-level rises.

Results from Multiple Stochastic Simulations

Figure 11 illustrates impacts of the different rates of sea-level rise on the evolution of the dune height and backshore shoreline position for profile 3. Figure 11a demonstrates slight sea-level rise effects on the dune height, since dune erosion and growth processes are not affected by the rate of sea-level rise. However, as shown in Figure 11b, the backshore shoreline position is significantly affected by the rates of sea-level rise. The profile grows under the first four scenarios but becomes narrower under the fifth scenario, which has the largest sea-level rise of 2 m. This indicates the importance of considering multiple sea-level rise scenarios to address scenario uncertainty. MC simulations were conducted for uncertainty quantification. Figure 12 shows that, to obtain stable estimates of sample statistics (e.g., mean and variance) that do not change with the number of MC simulations, 1000 simulations are sufficient over the domain during the entire simulation period under all five sea-level rise scenarios. The predictive uncertainty was quantified by examining the mean, variance, and probability density functions (PDFs) of the variables of interest, such as dune height and backshore position.

The predicted behaviors of the backshore position are presented as an example. Figure 13 illustrates temporal variation of the mean and variance of backshore position at profile 3 under five sea-level rise scenarios. Temporal varia-

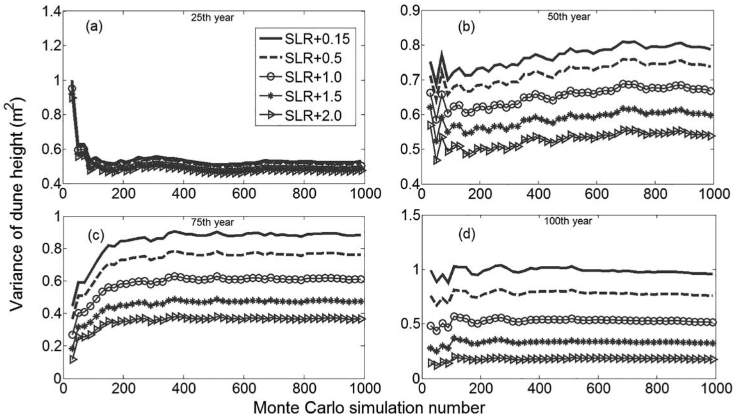

Figure 12. Convergence of sample variance of dune height with number of Monte Carlo simulations at profile 3 on the (a) 25th, (b) 50th, (c) 75th, (d) 100th year of the BIP model simulation.

tions of the mean and variance are distinct under different scenarios. The mean of the backshore position increases with time under the first three scenarios but decreases under scenarios SLR + 1.5 and SLR + 2.0. The variance increases with time under all five scenarios, which implies that the total predictive uncertainty increases with time, with the smallest increasing rate being that under scenario SLR + 0.15. This variability poses large predictive uncertainty, particularly under the scenarios of large sea-level rise and long simulation time. The PDFs of backshore position for the same profile are shown in Figure 14. The PDFs can be used for risk assessment, for example, the risk that backshore position is less than certain criterion of environmental protection and regulation. Figure 14 also shows that the patterns under different sea-level rise scenarios become more distinct with time increase, implying that scenario uncertainty increases with time. In addition, the PDFs of sea-level rise scenarios with larger rates have larger ranges. This explains the larger variance of the scenarios as shown in Figure 13. Decision-making or engineering design based on a single simulation or on the mean is risky, and the substantial variability should be addressed in coastal engineering design and long-term management. In comparison with the mean and variance, the PDFs are more comprehensive and quantitative for quantifying predictive uncertainty.

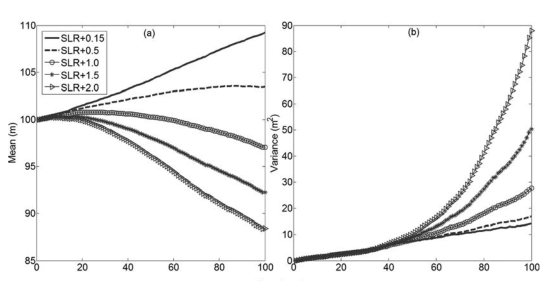

Figure 13. Temporal variation of (a) mean and (b) variance of backshore position of profile 3 under five sea-level rise scenarios.

DISCUSSION

The transfer of sand landward from the beach to the dunes and beyond to the island platform and backshore is essential to the maintenance of transgressive barrier islands. This has been well known for a long time. The BIP model quantifies the rates of sand transfer between the morphological elements of the barrier islands. The model demonstrates a first-order relationship of barrier island maintenance between sea-level rise and the storm climate. Storms periodically induce surge heights sufficient to cause dune erosion and overwash. Without these events, sand could not nourish the parts of the barrier islands inland of the coastal dunes. An adequate number of storms are needed to balance the inundation effect of sea-level rise and to provide the needed dune erosion volume to maintain the profiles of barrier islands.

The BIP model results provide insights into the barrier island dune evolution patterns under storm impacts. All of the dunes go through cycles of destruction and construction. The initial dune height is not a factor in the long-term dune evolution. Areas of low dunes are more susceptible to destruction, especially during periods where storms occur in

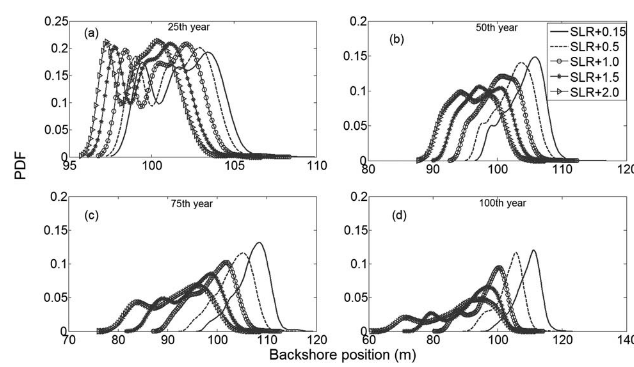

Figure 14. Probability density functions (PDFs) of backshore position at profile 3 on the (a) 25th, (b) 50th, (c) 75th, (d) 100th year of the BIP model simulation.

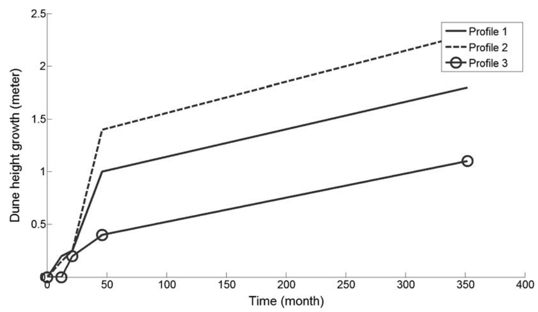

Figure 15. The dune heights evolution in 352 months after hurricane Alicia from three island profiles in the study of Morton, Paine, and Gibeaut (1994).

a close sequence. However, such sequences are rare, and eventually the dune growth allows the development of more stable larger dunes. Conversely, dunes can grow to a large size during rare episodes multiple years without storms, but eventually these are eroded. The overall result is that there is a dominance of a particular dune size given the storm climate, the annual rate of eolian sand transport from the beach, and rate of sea-level rise.

The model results confirm that the overwash sediment supply determines the erosion or accretion pattern of the back barrier, which leads to narrower or wider barrier islands. Similar conclusions have been made in some recent studies. Carruthers *et al*. (2013) estimated the overwash flux and used it to explain the barrier island evolution tendency; Timmons *et al*. (2010) pointed out that the high elevation and width of a barrier island can lead to insufficient overwash sediment and back-barrier erosion. In the BIP model results, a wide island width tends to trap the overwash sediment supply and cause back-barrier erosion. Houser and Hamilton (2009) found that the backshore accretion was indeed larger on the narrow island sections.

The dune recovery phenomenon can also be observed in the BIP model results, since there is constant eolian sediment transport into the dune in the model mechanism. Variant dune recovery patterns after hurricanes can be found in the research of Houser, Hapke, and Hamilton (2008); Houser and Hamilton (2009); Morton, Paine, and Gibeaut (1994); and Priestas and Fagherazzi (2010). The research of Morton, Paine, and Gibeaut (1994), conducted at Galveston Island, Texas, provided a relatively detailed time series of island profile evolution. Profile 1 to profile 3 in Morton, Paine, and Gibeaut (1994) contain obvious foredunes. The dune height growth values over a period of 352 months following Hurricane Alicia (1983) from three of these profiles are plotted in Figure 15. This shows that the dune growth patterns are similar in shape on all three island profiles: a relatively fast recovery of dune height is followed by progressively slower growth. This can also be found in the dune recovery patterns produced by the BIP model (Figure 10). This pattern is explained by the fact that more sediment is needed to build the same dune height increment when the dune base is wider (Figure 4). The dune growth rates in Figure 15 are from 1 to 2.3 m for 10 years. The fact that the BIP shows generally similar dune growth rates indicates that the bulk onshore eolian transport rate of 1.3 m^3/m/y is reasonably representative for a Gulf Coast environment. Another research project conducted on the Santa Rosa Island, Florida after 2005 hurricane Ivan also demonstrated a similar dune averaging recovery rate of approximately 0.1 to 0.3 m/y (Bambach, 2013). Some other profiles in the Morton, Paine, and Gibeaut (1994) research show different dune recovery patterns. This spatial variation of dune recovery observed in reality is due to different sediment source, dune formation, and geographic reasons that are not resolved in the BIP model. In the future the BIP model could be modified to include more detailed representations of the eolian sand flux to coastal dunes.

Although the model simulations of the semisynthetic barrier island profiles did not explicitly include calibrations to actual time histories of the Santa Rosa Island examples, the simulated patterns of dune erosions under storms qualitatively agree with the patterns observed at Santa Rosa Island. For example, Claudino-Sales, Wang, and Horwitz (2010) showed that, after hurricane Ivan occurred in September 2004, the front beach dunes along two profiles located in the middle segment (FP2) of Fort Pickens State Park on Santa Rosa Island were completely eroded. The pattern of complete erosion is simulated on several profiles (Figure 10) in this study. Among the profiles, profile 1 most resembles the two FP2 profiles in terms of the distance between storm tracks and profile locations, profile dune heights, and island width along the profiles. Figure 10a shows that the dune along profile 1 is completely removed at year 21, when a magnitude 3 storm occurs along track 3. The similar match between observed and simulated patterns of barrier island geomorphological evolutions can also be found for hurricane Dennis, which occurred in July 2005 (Claudino-Sales, Wang, and Horwitz, 2008). These results suggest that the BIP model helps understand long-term responses of barrier island geomorphology to future storms. It is expected that, after calibrating the BIP model with field data, the BIP model design may be used as a vital tool for coastal management and protection with consideration of long-term climate impacts.

The BIP model results clearly demonstrate the importance of storm sequence on the cross-shore morphology of barrier islands. The use of a Poisson distribution to define the annual rate of hurricane occurrence is well established (Niedoroda *et al*., 2010; Resio, 2007), and its use in the BIP model shows that sequences of two or more major storms within a few years is rare. The model demonstrates that island relief is suppressed during these periods but that the island profiles recover in the subsequent periods of less frequent storms. This is an important observation in the management of barrier islands, since it can forestall any overreaction by government and private interests.

This barrier island modeling study also demonstrates that scenario uncertainty becomes increasingly important with time (Figure 14). A similar trend was reported in the regional climate modeling of Hawkins and Sutton (2009, 2011), who simulated surface temperature at the global scale with three different CO_2 emission scenarios from 2000 to 2010. Their modeling results suggest that scenario uncertainty accounts for 80% of total predictive uncertainty after a 90-year simulation of certain areas such as SE Asia. A similar pattern was also reported during research of global mean temperature prediction (Cox and Stephenson, 2007), which suggests that scenario uncertainty dominates in the total uncertainty after 30–50 years of prediction time. Therefore, to reduce predictive uncertainty, resources should be spent to screen and/or narrow plausible scenarios in long-term modeling of both barrier island evolution and future climates.

The current BIP model is subject to several limitations, and more model development is warranted in future studies. Although the BIP model represents the major morphological features of barrier island profiles, several important processes and features have either been generalized or left out of the conceptual model completely. The most significant of these is the role of vegetation in stabilizing dunes and promoting their growth. All of the wind-blown sand that impinges on the dunes is assumed to remain there, and this assumption partially represents one of the effects of dune vegetation. However, subsequent versions of the model should include a more detailed representation of dune vegetation and its impact on dune stability. The beach prism in the BIP model is assumed to track the sea-level rise, and its volume is maintained as a constant value. As it stands now, the BIP model represents the relative changes in the dimensions of barrier island morphological features without regard to the geographic coordinates. In reality the beach prism volume must be maintained by spatial gradients in the longshore transport of sand in the surf zone, or the whole profile must shift due to long-term accretion or erosion of the shoreline. These effects are absent from the present version of the model. This problem can be solved by incorporating the longshore sediment transport in the manner of Niedoroda *et al*. (1995), and this model development is currently underway.

In its present form the BIP model is limited to representing natural portions of barrier islands that are not impacted by development or erosion defense structures. It is envisioned that the time-, and space-average effects of such developments could be created and incorporated in a future model version in a manner similar to that provided by the barrier–resort model of McNamara and Werner (2008).

The BIP model can only provide averaged (e.g., 250 m in space and annual in time) responses of barrier islands to storms. Other models such as those developed by Roelvink *et al*. (2009) and Reed *et al*. (2011) can provide greater detail but are not well suited to simulate the very large number of realizations of long-term storm sequences that can be resolved by the BIP model.

CONCLUSION

The BIP model presented in this paper provides a useful tool for predicting barrier island evolution under the impacts of multiple possible future climate scenarios. The modeling results demonstrate that the BIP model, using relatively simple representations of time- and space-averaged processes, is capable of simulating realistic patterns of barrier island profile evolution over time spans of a century. The BIP model also allows the rate of backshore retreat as a function of island width in light of accelerated sea-level rise to be quantified and also related to the frequency and intensity of hurricanes as well as proximity of hurricane landfalls to island profiles. In the BIP model, the time-averaged rate of sand transfer from the beach prisms and dunes to the backshore is balanced against the inundation effects of sea-level rise.

The BIP modeling results reveal that the initial conditions of dune profiles control dune evolution for a period of about four to five decades. After this period, different dunes tend to converge to a dominant size, and this tendency is controlled by a time-averaged sediment transport processes. In addition, the BIP model addresses uncertainty in future storm events and rates of sea-level rise. It is demonstrated in this study that the uncertainty in projecting barrier island evolution is significant. The predictive uncertainty substantially increases with time and sea-level rise rates; the contribution of uncertainty in sea-level rise to predictive uncertainty increases with time.

The BIP model provides a pilot example of simplified modeling of barrier island evolution considering uncertainty of future climate impacts. Future study will be focused on expanding the BIP model algorithms to include time-averaged representations of longshore processes and response. This will allow a more complete simulation of the historic changes on Santa Rosa Island, comprehensive predictions of its future change under different sea-level rise scenarios, and a proper representation of the uncertainty associated with these predictions.

ACKNOWLEDGMENTS

This research is supported in part by the DoD Strategic Environmental Research and Development Program (SERDP) through contract number SERDP RC-1700 and by the DOE Early Career Award, DE-SC0008272, to the second author.

LITERATURE CITED

Bambach, P.W., 2013. Dune and Shoreline Evolution of Western Santa Rosa Island, Florida, 1973–2013. Tallahassee, Florida: Florida State University, Master's thesis, 64p.

Bauer, B.O. and Davidson-Arnott, R.G.D., 2002. A general framework for modeling sediment supply to coastal dunes including wind angle, beach geometry, and fetch effects. *Geomorphology*, 49, 89–108.

Carruthers, E.A.; Lane, D.P.; Evans, R.L.; Donnelly, J.P., and Ashton, A.D., 2013. Quantifying overwash flux in barrier systems: An example from Martha's Vineyard, Massachusetts, USA. *Marine Geology*, 343, 15–28.

Claudino-Sales, V.; Wang, P., and Horwitz, M.H., 2008. Factors controlling the survival of coastal dunes during multiple hurricane impacts in 2004 and 2005: Santa Rosa barrier island, Florida. *Geomorphology*, 95(3–4), 295–315.

Claudino-Sales, V.; Wang, P., and Horwitz, M.H., 2010. Effects of Hurricane Ivan on Coastal Dunes of Santa Rosa Barrier Island, Florida: Characterized on the Basis of Pre- and Poststorm LIDAR Surveys. *Journal of Coastal Research*, 26(3), 470–484.

Cox, P. and D. Stephenson, 2007. A changing climate for prediction. *Science*, 317, 207–208. doi:10.1126/science.1145956

De Vriend, H.J., 1991. Mathematical modeling and large-scale coastal behavior. *Journal of Hydraulic Research*, 29(6), 727–740.

De Vriend, H.J.; Capobianco, M.; Chesher, T.; De Swart, H.E.; Latteux, B., and Stive, M.J.F., 1993. Approaches of long-term modelling of coastal morphology: A review. *Coastal Engineering*, 21, 225–269.

Donnelly, C.; Kraus, N., and Larson, M., 2006. State of knowledge on measurement and modeling of coastal overwash. *Journal of Coastal Research*, 22(4), 965–991.

Duran, O. and Moore, L.J., 2013. Vegetation controls on the maximum size of coastal dunes. *Proceedings of the National Academy of Sciences*, 110, 17,217–17,222.

FEMA (Federal Emergency Management Agency) Staff, 2002. Flood Insurance Study, Okaloosa County, Florida and unincorporated areas. Washington, D.C.: FEMA, *Flood Insurance Study, number 12091CV000A*.

Godfrey, P.J. and Godfrey, M.M., 1976. *Barrier Island Ecology of Cape Lookout National Seashore and Vicinity, North Carolina*. National Park Service Scientific Monograph Series, Publication No. 9. Washington, D.C.: U.S. Government Printing Service.

Grinsted, A.; Moore J.C., and Jevrejeva, S., 2010. Reconstructing sea level from paleo and projected temperatures 200 to 2100 AD. *Climate Dynamics*, 34, 461–472.

Hanson, H.; Larson, M., and Kraus, N.C., 2010. Calculation of beach change under interacting cross-shore and longshore processes. *Coastal Engineering*, 57, 610–619.

Hawkins, E. and Sutton, R., 2009. The potential to narrow uncertainty in regional climate predictions. *Bulletin of American Meteorological Society*, 90, 1095–1107.

Hawkins, E. and Sutton, R., 2011. The potential to narrow uncertainty in projections of regional precipitation change. *Climate Dynamics*, 37, 407–418.

Houser, C. and Hamilton, S., 2009. Sensitivity of post-hurricane beach and dune recovery to event frequency. *Earth Surface Processes and Landforms*, 34, 613–628.

Houser, C.; Hapke, C., and Hamilton, S., 2008. Controls on coastal dune morphology, shoreline erosion and barrier island response to extreme storms. *Geomorphology*, 100, 223–240.

Houser, C.; Hobbs, C., and Saari, B., 2008. Posthurricane airflow and sediment transport over a recovering dune. *Journal of Coastal Research*, 24(4), 944–953.

IPCC (Intergovernmental Panel on Climate Change), 2007. *Climate Change 2007: The Physical Science Basis*. Contribution of Working Group I to the Fourth Assessment Report of the Intergovernmental Panel on Climate Change. Cambridge, U.K.: Cambridge University Press, 996p.

Jelesnianski, C.P.; Chen, J., and Shaffer, W.A., 1992. SLOSH: Sea, Lake and Overland Surges from Hurricanes. *NOAA Technical Report NWS 48*. Washington, D.C.: NOAA.

Jevrejeva, S.; Moore J.C., and Grinsted, A., 2010. How will sea level respond to changes in natural and anthropogenic forcings by 2100? *Geophysics Research Letter*, 37, L07703. doi:10.1029/2010GL042947

Kish, S.A. and Donoghue, J.F., 2013. Coastal response to storms and sea-level rise: Santa Rosa Island, Northwest Florida, U.S.A. In: Brock, J.C.; Barras, J.A., and Williams, S.J. (eds.), *Understanding and Predicting Change in the Coastal Ecosystems of the Northern Gulf of Mexico*. Journal of Coastal Research, Special Issue No. 63, pp. 131–140.

Larson, M.; Erikson, L., and Hanson, H., 2004. An analytical model to predict dune erosion due to wave impact. *Coastal Engineering*, 51, 675–696.

Larson, M.; Kraus, N.C., and Connell, K.J., 2006. Modeling sediment storage and transfer for simulation regional coastal evolution. *Proceedings of the 30th Coastal Engineering Conference*, (San Diego, California, ASCE), pp. 1–13.

McNamara, D.E. and Werner, B.T., 2008. Coupled barrier island-resort model, 1: Emergent instabilities induced by strong human-landscape interactions. *Journal of Geophysical Research*, 113, F01016. doi: 10.1029/2007JF000840

Miller, D. L.; Thetford, M.; Dupree, J., and Atwood, L., 2014. Influence of seasonal changes and shifting substrate on survival of restoration planting of *Schizachyrium maritimum* (Gulf bluestem) on Santa Rosa Island, Florida. *Journal of Coastal Research*, 30(2), 237–247.

Morton, R.A., 2002. Factors controlling storm impacts on coastal barriers and beaches—A preliminary basis for near real-time forecasting. *Journal of Coastal Research*, 18(3), 486–501.

Morton, R.A.; Paine, J.G., and Gibeaut, J.C., 1994. Stages and durations of post-storm beach recovery, southeastern Texas coast. *Journal of Coastal Research*, 10(4), 884–908.

Niedoroda, A.W.; Reed, C.W.; Swift, D.J.P.; Arata, H., and Hoyanagi, K., 1995. Modeling shore-normal large-scale coastal evolution. *Marine Geology*, 126, 181–199.

Niedoroda, A.W.; Resio, D.T.; Toro, G.R.; Divoky, D.; Das, H.S., and Reed, C.W., 2010. Analysis of the Coastal Mississippi Storm Surge Hazard. *Ocean Engineering*, 37, 82–90.

NRC (National Research Council), 1987. *Responding to Changes in Sea Level: Engineering Implications*. Washington, D.C.: National Academy Press, 160p.

Priestas, A.M. and Fagherazzi, S., 2010. Morphological barrier island changes and recovery of dunes after hurricane Dennis, St. George Island, Florida. *Geomorphology*, 114, 614–626.

Reed, C.W.; Brown, M.E.; Sanchez, A.; Wu, W., and Buttolph, A.M., 2011. The coastal modeling system flow model (CMS-Flow): Past and Present. *In:* Rosati, J.D.; Wang, P., and Roberts, T.M. (eds.), *Proceedings, Symposium to Honor Dr. Nicholas C. Kraus*, Journal of Coastal Research, Special Issue No. 59, pp. 1–6.

Resio, D.T., 2007. White paper on estimating inundation probabilities. Vicksburg, Mississippi: U.S. Army Corps of Engineers, Engineering Research and Development Center.

Roelvink, D.; Reniers, A.D.; van Dongeren, A.P.; van Thiel de Vries, J.; McCall, R., and Lescinski, J., 2009. Modelling storm impacts on beaches, dunes and barrier islands. *Coastal Engineering*, 56, 1133–1152.

Sallenger, A.H., 2000. Storm impact scale for barrier islands. *Journal of Coastal Research*, 16(3), 890–895.

Stive, M.J.F., and De Vriend, H.J., 1995. Modelling shoreface profile evolution. *Marine Geology*, 126, 235–248.

Stive, M.J.F.; Nicholls, R.J., and De Vriend, H.J., 1991. Sea-level rise and shore nourishment: A discussion. *Coastal Engineering*, 16(l), 147–163.

Stone, G.W.; Liu, B.; Pepper, D.A., and Wang, P., 2004. The importance of extratropical and tropical cyclones on the short-term evolution of barrier islands along the northern Gulf of Mexico, USA. *Marine Geology*, 210, 63–78.

Taylor Engineers, 2007. *Okaloosa Island Beach Management Feasibility Study*. Okaloosa County, Florida: Unpublished consulting report, 109p.

Timmons, E.A.; Rodriguez, A.B.; Mattheus, C.R., and DeWitt, R., 2010. Transition of a regressive to a transgressive barrier island due to back-barrier erosion, increased storminess, and low sediment supply: Bogue Banks, North Carolina, USA. *Marine Geology*, 278, 100–114.

USACE (U.S. Army Corps of Engineers), 1984. *Shore Protection Manual Volume 1*. Washington, D.C.: U.S. Government Printing Office.

USACE, 1998. *Coastal Engineering Manual*. Washington, D.C.: U.S. Government Printing Office.

Vermeer, M. and Rahmstorf, S., 2009. Global sea level linked to global temperature. *Proceedings of the National Academy of Sciences*, 106(51), 21,527–21,532. doi:10.1073/pnas.0907765106

Wang, P.; Kirby, J.H.; Haber, J.D.; Horwitz, M.H.; Knorr, P.O., and Krock, J.R., 2006. Morphological and sedimentological impacts of Hurricane Ivan and immediate post-storm beach recovery along the northwestern Florida barrier-island coasts. *Journal of Coastal Research*, 22(6), 1382–1402.